International Journal of Innovative Technology and Exploring Engineering (IJITEE)
ISSN: 2278-3075 (Online), Volume-4 Issue-6, November 2014

Enhanced Room Temperature Ferromagnetism in Polyethylene Glycol Capped $Sn_{0.99-x}Cu_xCr_{0.01}O_2$ Nanoparticles

K. Subramanyam, N. Sreelekha, D. Amaranatha Reddy, G. Murali, R. P. Vijayalakshmi

***Abstract* — $Sn_{0.99-x}Cu_xCr_{0.01}O_2$ *(x=0.00, 0.01, 0.03, 0.05 and 0.07) nanoparticles were synthesized by simple chemical co-precipitation method using polyethylene glycol (PEG) as a surfactant for the first time. EDAX spectra confirmed the presence of Cr and Cu in the host material with near stoichiometric ratio. The results from XRD studies indicated that the synthesized samples had a single phase rutile type tetragonal crystal structure as that of (P4₂/mnm)* SnO_2*. TEM analysis revealed that the average particle size lies in the range of 8-10 nm. Optical absorption spectra and corresponding Tauc's plots showed a blueshift in optical absorption band edge, the bandgap widening with increasing Cu concentration in* $Sn_{0.99-x}Cu_xCr_{0.01}O_2$ *nanoparticles can be well explained in terms Burstein–Moss effect. From magnetization measurements it is noticed that the saturation magnetization increases for 1% of Cu doping, then decreased with increasing the Cu concentration. The observed magnetic behavior is well supported with the bound magnetic polarons (BMPs) model.*

***Keywords:** Cu co-doping, chemical synthesis, Burstein–Moss effect, FTIR spectra, Room temperature ferromagnetism.*

I. INTRODUCTION

Dilute magnetic semiconductors (DMSs) are promising materials for the new functionality of memory devices, detectors, light emitting sources and possible use in next generation spintronic devices with enhanced functionalities such as spin valve transistors, spin light emitting diodes, non-volatile storage and logic devices, since they possess charge and spin degrees of freedom in single substance [1-4]. Recently, extensive research has been performed on transitional metal doped oxide based dilute magnetic semiconducting systems, with the major focus on creating room temperature ferromagnetic semiconductors at above the room temperature [5-9]. Among the family of oxide based semiconductors, SnO_2 is a technologically versatile and important semiconducting material for many applications especially in nanocrystalline form such as gas sensors, optoelectronic devices, dye based solar cells, liquid crystal display transistors and secondary lithium batteries owing to its wide bandgap (3.6 eV at 300 K), relatively large excitation binding energy and good optical transparency in the visible region [10-15]. Further, up to now a numerous results are reported by several research groups on single transition metal ion doped SnO_2 DMS nanoparticles synthesized by different methods [5, 16-21], but doping of two different kinds of ions simultaneously in a host material generates magnetic property which is quite different from the magnetic property developed due to presence of single transition metal ion, this property is very useful for spintronic applications [22, 23]. Further, co-doping is a fairly simple and effective method to amend the number of vacancies and interstitial host metal atoms, which is useful to explore the mechanism of RTFM. On the other hand, co-doping under appropriate conditions can modify the intrinsic point defects of the TM-doped DMS and influence the properties of the carriers to regulate the magnetism [22, 23]. Moreover to the best of our knowledge, very few co-doped SnO_2 systems have also been reported with expectation that co-doping can lead to remarkable changes in the properties of the materials. K. Nomura et al. [22] found enhanced room temperature ferromagnetism in Fe and Co co-doped SnO_2. Jun Okabayashi et al. [23] reported enhanced room temperature ferromagnetism in Fe and Mn co-doped SnO_2. Jasneet Kaur et al. [24] reported electrical and magnetic properties of Co and Fe doped SnO_2 nanorods by Ce co-doped. S. Dalui et al. [25] observed room temperature ferromagnetism in (Co, Mo): SnO_2 films prepared by pulsed laser deposition. In the previous work, we have reported a systematic study on the structural, optical and magnetic properties of Cr doped SnO_2 nanoparticles and observed well defined RTFM hysteresis loop for 1% Cr concentration [26]. In order to study the effect of Cu co-doping, in this paper we report the synthesis, structural, optical and magnetic properties of $Sn_{0.99-x}Cu_xCr_{0.01}O_2$ (x= 0.00, 0.01, 0.03, 0.05 and 0.07) nanoparticles by the simple chemical co-precipitation method using polyethylene glycol (PEG) as a template. Here we chose Cr and Cu as doping elements, because unlike many other metals, Cr itself is anti-ferromagnetic and an extrinsic ferromagnetism cannot be induced even if Cr clustering occurs [27]. In addition, Cu is a preferred choice to avoid controversies since the secondary phases such as CuO, Cu_2O or Cu related clusters could not contribute to the room temperature ferromagnetism [28], as well as the ionic radii of Cr^{3+} (0.063 nm) and Cu^{2+} (0.065 nm) metal ions are very close to the ionic radius of Sn^{4+} (0.069 nm) metal ion. Among the different kinds of capping agents, here the water soluble PEG was used as a capping agent, it has attracted great attention, because polymer molecules adsorbs to the nanoparticle surface, is generally added both to control the size of the nanoparticles and to prevent the agglomeration of the synthesized particles and it is bio-compatible [29].

Manuscript published on 30 November 2014.
***Correspondence Author(s)**
R. P. Vijayalakshmi, Department of Physics, Sri Venkateswara University, Tirupati, India.
K. Subramanyam, Department of Physics, Sri Venkateswara University, Tirupati, India.

II. EXPERIMENTAL

$Sn_{0.99-x}Cu_xCr_{0.01}O_2$ (x=0.00, 0.01, 0.03, 0.05 and 0.07) nanoparticles capped with PEG were synthesized by simple co-precipitation method. All the chemicals $SnCl_4.5H_2O$, $CrCl_3.6H_2O$, $CuCl_2.6H_2O$ and NH_4OH used in the present study are of AR grade (Sigma Aldrich 99.99%) and used without further purification. Aqueous solutions of precursors (0.2M) were separately prepared as per stoichiometric ratio and stirred for 30 min. In this solution NH_4OH (28%) solution was added drop wise in very controlled manner to maintain the chemical homogeneity. The addition of NH_4OH was stopped when pH of the solution reached to 9 at room temperature and added 2ml of surfactant (PEG-400) under vigorous stirring for 8 hr. The precipitate was filtered out separately and washed with de-ionized water to remove unnecessary impurities formed during the synthesis process. The obtained product was placed in oven for 14 hr at 60^0 C and the dried samples were grounded for half an hour and then annealed at 450^o C for 3 hr to obtain $Sn_{0.99-x}Cu_xCr_{0.01}O_2$ nanoparticles. The samples of $Sn_{0.99-x}Cu_xCr_{0.01}O_2$ (x= 0.00, 0.01, 0.03, 0.05 and 0.07) were subjected to various characterization studies. Structural investigations were done by ''Seifert 3003 TT X-ray Diffractometer'' with Cu-Kα radiation with a wavelength of 1.542 Å. Crystal structure and crystallite size were obtained from XRD data. The particle size and structure confirmations were done by Phillips TECHNAI FE 12, Transmission Electron Microscope (TEM). The optical absorption measurements were performed in (JASCO-V-670) spectrophotometer. FTIR studies were carried out using Thermo Nicolet FTIR-200 thermo Electron Corporation. Room temperature magnetization was recorded using a Lakeshore Vibrating Sample Magnetometer, VSM 7410.

III. RESULTS AND DISCUSSION

A. Elemental Analysis

In order to confirm the presence of Cr and Cu ions in the host material, the EDAX spectra of co-doped samples were recorded. Fig.1 shows the EDAX spectra of $Sn_{0.99-x}Cu_xCr_{0.01}O_2$ (x=0.01) nanoparticles. The EDAX spectra exhibited signals corresponding to Sn, O, Cr and Cu only, indicated that the nanoaprticles are made up of tin, oxygen, chromium and cupper and no other impurity elements are found within the detection limit of the instrument.

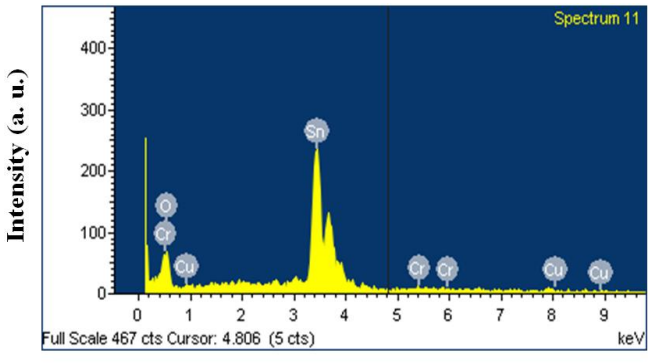

Fig. 1 EDAX Spectra of $Sn_{0.99-x}Cu_xCr_{0.01}O_2$ (x= 0.01) Nanoparticles

B. Structural Analysis

The as synthesized samples were subjected to XRD studies to obtain information about the crystallinity, size and phase of the $Sn_{0.99-x}Cu_xCr_{0.01}O_2$ (x= 0.00, 0.01, 0.03, 0.05 and 0.07) nanoparticles. Fig. 2 represents the XRD patterns of $Sn_{0.99-x}Cu_xCr_{0.01}O_2$ (x=0.00, 0.01, 0.03, 0.05 and 0.07) nanoparticles and all the peaks could be indexed to the rutile type tetragonal crystal structure of SnO_2 with space group ($P4_2/mnm$). The peaks observed in the XRD patterns match well with the standard JCPDS file no. (41-1445) of SnO_2. No additional peaks corresponding to the possible impurity phases were observed in the XRD pattern. It is also found that the XRD peaks become gradually sharper with increasing the doping concentration indicating the increase of particle size. The average crystallite size of $Sn_{0.99-x}Cu_xCr_{0.01}O_2$ (x= 0.00, 0.01, 0.03, 0.05 and 0.07) nanoparticles were determined from XRD broadening using the Debye-Scherer formula, $D=0.89\lambda/\beta\cos\theta$, where λ is the wavelength of X-ray radiation, β is the full width at half maximum of the peak at diffraction angle θ [30] and the average grain sizes are found to be in the range of 6-8 nm. The increase of crystallite size with increasing the doping concentration may be attributed to the micro structural changes due to non uniform stress or strain during the grain growth or to the existence of local structural disorder in the material at the time of formation. Jun Okabayashi et al. [23] also reported similar increase in crystallite size by co-doping of (Fe, Mn) ions in SnO_2.

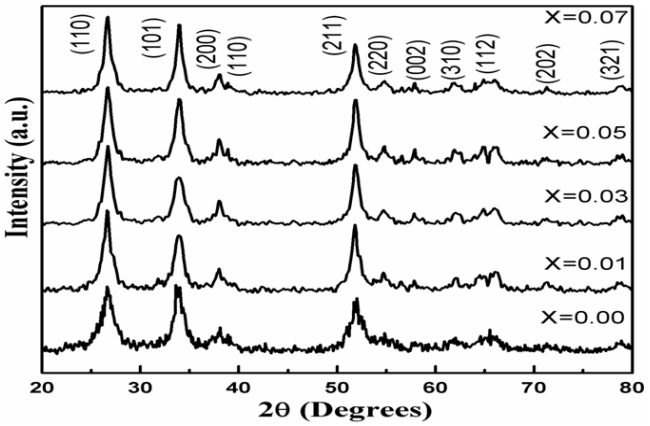

Fig. 2 XRD Patterns of Sn0.99-xCuxCr0.01O2 Nanoparticles

C. TEM, HRTEM and SAED Analyses

To obtain the particle size and the information about the nanostructures by direct measurement, TEM is a powerful instrument, it can reveal the size and morphology of the nanoparticles. Fig. 3 shows typical TEM images of $Sn_{0.99-x}Cu_xCr_{0.01}O_2$ (x=0.00, 0.01, 0.03, and 0.05) nanoparticles. Powder samples were dispersed in ethanol and sonicated in ultrasonic bath for 15 min for TEM analysis. It was obvious from the TEM micrograph that the morphology of the particles are found to be nearly spherical in shape and from the images it is also evident that in the present synthesized samples agglomeration was decreased with uniform distribution of particles by the addition of PEG to the host matrix.

Published By:
Blue Eyes Intelligence Engineering
and Sciences Publication (BEIESP)

The average size of nanoparticles obtained from TEM analysis is about 10 nm which is good agreement with the XRD results and it was clearly confirmed by particle size distribution plots as shown in Fig. 4. Fig. 5 (a-c) show the HRTEM image of $Sn_{0.99-x}Cu_xCr_{0.01}O_2$ (x=0.00, 0.03 and 0.05) nanoparticles are about 5 nm with clear lattice fringes. Fig. 5 (d) explore the selected area electron diffraction (SAED) pattern of the $Sn_{0.99-x}Cu_xCr_{0.01}O_2$ (x=0.01) sample and all crystalline rings could be indexed to a rutile type of SnO_2 tetragonal crystal structure.

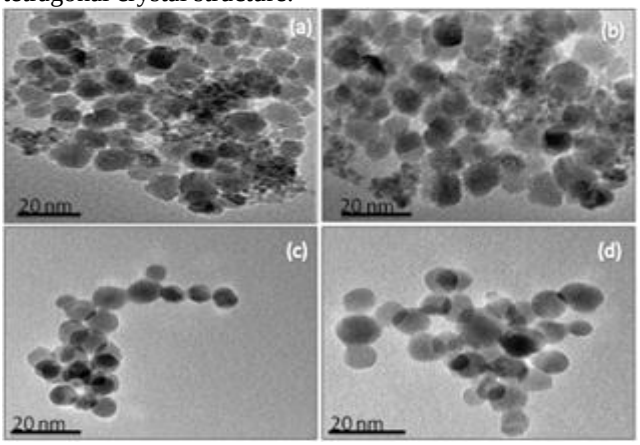

Fig. 3 (a-d) TEM Images of Sn0.99-xCuxCr0.01O2 (x= 0.00, 0.01, 0.03 and 0.05) Nanoparticles

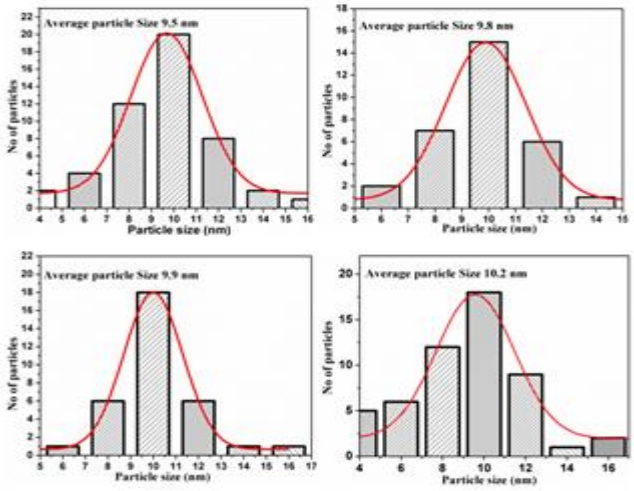

Fig. 4 Particle Size Distribution Graphs for Sn0.99-xCuxCr0.01O2 (x= 0.00, 0.01, 0.03 and 0.05) Nanoparticles

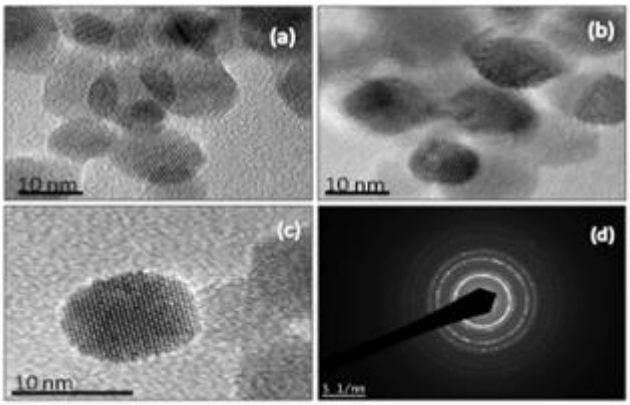

Fig. 5 (a-c) HRTEM Images of the Sn0.99-xCuxCr0.01O2 (x= 0.00, 0.03 and 0.05) Nanoparticles. (d) SAED Pattern of Sn0.99-xCuxCr0.01O2 (x=0.01) Nanoparticles

D. Optical absorption studies

UV-vis optical absorption spectroscopy is a constructive technique for the characterization of synthesized DMS nanoparticles to get the information of optical bandgap values. The optical absorption spectra and corresponding Tauc's plots of $Sn_{0.99-x}Cu_xCr_{0.01}O_2$ (x= 0.00, 0.01, 0.03, 0.05 and 0.07) nanoparticles are shown in Fig. 6 and Fig. 7 respectively. Absorption spectra shows an ultraviolet cut-off wavelength around 285–305 nm, which can be different samples varies as the concentration of Cu in the $Sn_{0.99-x}Cu_xCr_{0.01}O_2$ nanoparticles varies. In order to calculate the direct bandgap, we used the Tauc's relation, $\alpha h\nu = A(h\nu - Eg)^n$, Where α is the absorption coefficient, A is a constant and n=1/2 for direct bandgap semiconductor. An extrapolation of the linear region of a plot of $(\alpha h\nu)^2$ vs $h\nu$ gives the value of the optical band gap. The measured bandgap was found to be 4.21 eV for 1% Cr doped SnO2 nanoparticles, which is higher than the reported value of the bulk SnO_2 (3.6 eV) [31]. This can be attributed to the strong quantum confinement of the nanoparticles. On doping of Cu in to the $Sn_{0.99-x}Cu_xCr_{0.01}O_2$ system, the bandgap energy increases, even though the particle size increases. Estimated bandgap values of $Sn_{0.99-x}Cu_xCr_{0.01}O_2$ nanoparticles with x = 0, 0.01, 0.03, 0.05 and 0.07 are 4.21 eV, 4.23 eV, 4.24 eV, 4.26 eV and 4.32 eV respectively. Widening of bandgap with increasing Cu content can be well explained in terms of the so-called Burstein–Moss effect that the Fermi level merges into the conduction band with the increasing carrier concentration [32]. S. Dalui et al. [25] reported similar widening of bandgap in (Co, Mo): SnO2 films prepared by pulsed laser deposition. There is no data available on optical bandgap studies of $Sn_{0.99-x}Cu_xCr_{0.01}O_2$ (x= 0.00, 0.01, 0.03, 0.05 and 0.07) nanoparticles for comparison.

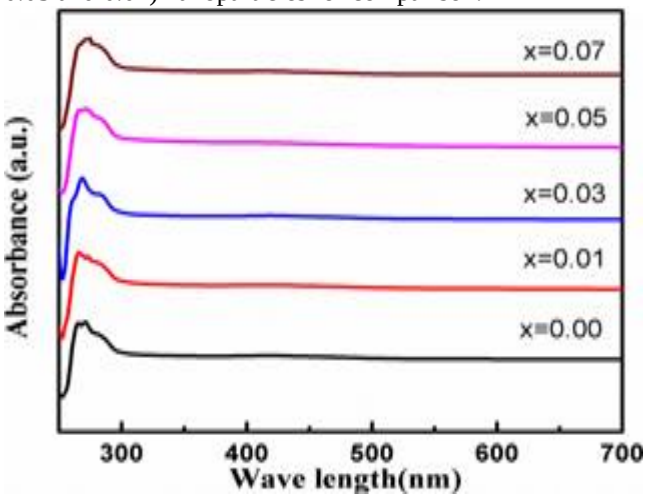

Fig. 6 Optical Absorption Spectra of the Sn0.99-xCuxCr0.01O2 (x= 0.00, 0.01, 0.03, 0.05 and 0.07) Nanoparticles

Published By:
Blue Eyes Intelligence Engineering
and Sciences Publication (BEIESP)

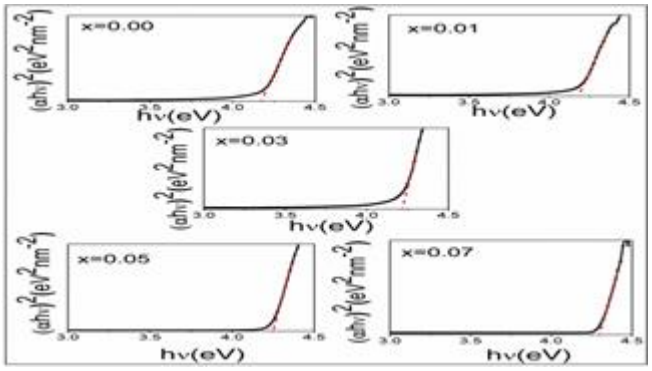

Fig. 7 Tauc's Plots of the Sn0.99-xCuxCr0.01O2 (x= 0.00, 0.01, 0.03, 0.05 and 0.07) Nanoparticles

E. FTIR Analysis

In order to confirm the phase purity of the investigated samples, FTIR was recorded in the range of 500 to 4000 cm-1. Due to larger probing depth of IR, this technique is more sensitive than X-ray diffraction and Raman spectroscopy in the characterization of phases and lattice distortions. Fig. 8 shows FTIR spectrum of $Sn_{0.99-x}Cu_xCr_{0.01}O_2$ (x= 0.00, 0.01, 0.03, 0.05 and 0.07) nanoparticles capped with PEG. All the samples exhibited absorption bands at 3741 cm^{-1}, 3614 cm^{-1}, 2943 cm^{-1}, 2310 cm^{-1}, 1672 cm^{-1}, 1508 cm^{-1}, 1095 cm^{-1} and 680-590 cm^{-1}. The spectral bands at 3741 cm-1, 3614 cm-1 and 1672 cm-1 are attributed to characteristic absorption of O-H stretching vibrations of H_2O molecule. The presence of these bands in synthesized nanoparticles may be due to the adsorption of atmospheric water content. A small absorption peak observed at 2943 cm^{-1} was due to C-H stretching vibrations. The spectral band at 2310 cm^{-1} is related with the $N\text{-}H^{3+}$ asymmetric stretching vibrations of amines. The absorption peaks found at 1508 cm^{-1} and 1095 cm^{-1} are assigned to the asymmetric and symmetric C-O stretching vibrations. Finally broad peak at around 680-590 cm^{-1} in Cr doped and (Cr, Cu) doped SnO_2 samples in the infrared spectra is due to the stretching vibrations of O-Sn-O it confirms the bonding of metal-oxygen as present in SnO_2 [33-36]. Fig. 9 shows FTIR spectra for uncapped SnO2 nanoparticles. The peaks are only located at 610 cm^{-1}, 1656 cm^{-1} and 1550 cm^{-1}. These peaks are related to metal-oxygen and hydroxyl compound. We have not observed any modes corresponding to the Cr and Cu, since it is located in the interior of the nanoparticle not on the surface. It is further indicated that Cr and Cu is completely doped into SnO_2. Further above considerations perceptibly confirmed that the surface of SnO_2: (Cr, Cu) nanoparticles were capped by PEG.

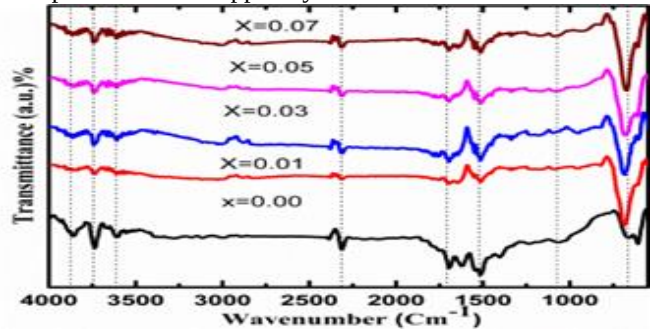

Fig. 8 FTIR Spectra of Sn0.99-xCuxCr0.01O2 (x= 0.00, 0.01, 0.03, 0.05 and 0.07) Nanoparticles

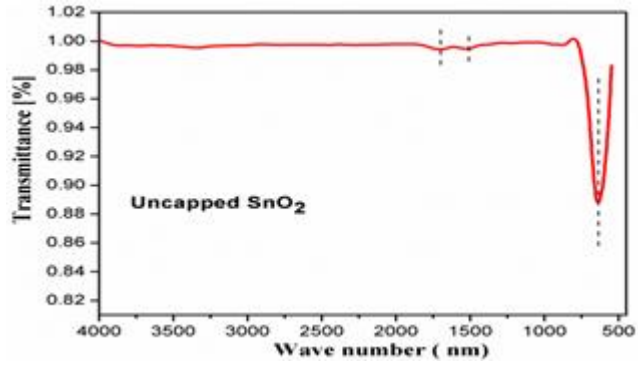

Fig. 9 FTIR Spectra of Uncapped SnO2 Nanoparticles

F. Magnetic Studies

Magnetization measurements were carried out at room temperature for $Sn_{0.99-x}Cu_xCr_{0.01}O_2$ (x= 0.00, 0.01, 0.03, 0.05 and 0.07) nanoparticles are as shown in Fig. 10. It is interesting to note that all the samples of the present investigation are found to exhibit room temperature ferromagnetism (RTFM). The room temperature ferromagnetism in Cr and Cu co-doped SnO_2 nanoparticles could arises by the number of secondary phases such as magnetic phase of CrO_2 or anti-ferromagnetic phases of Cr_2O_3, Cr_3O_4 or CuO, Cu_2O and Cu clusters. In fact no trace of Cr metal clusters and Cu related clusters was detected by XRD measurements in the synthesized nanoparticles, moreover none of them exhibited room temperature ferromagnetism above room temperature. Consequently it may conclude that the observed ferromagnetism in the present samples is not due to the presence of any secondary phases, and it is attributed to the doping of Cr, Cu metal ions and presence of oxygen vacancies in SnO_2 lattice. In case of $Sn_{0.99-x}Cu_xCr_{0.01}O_2$ (x= 0.00, 0.01, 0.03, 0.05 and 0.07) nanoparticles, the origin of ferromagnetism is very complex. Although different mechanisms might be responsible, an endeavor has been made to explain the phenomenon using bound magnetic polarons (BMPs) model [37, 38].

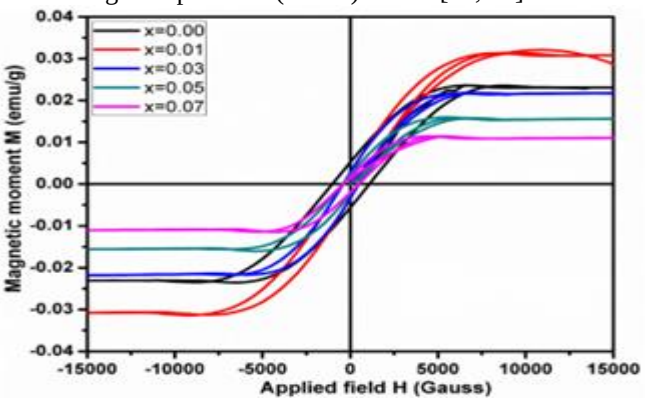

Fig. 10 Room Temperature M-H Plots of $Sn_{0.99-x}Cu_xCr_{0.01}O_2$ (x= 0.00, 0.01, 0.03, 0.05 and 0.07) Nanoparticles

According to BMP model, the localized spins of the dopant ions interact with the charge carriers which are bound to a small number of defects such as oxygen vacancies, resulting in a magnetic polarization of the surrounding local moments.

Published By:
Blue Eyes Intelligence Engineering and Sciences Publication (BEIESP)

In the samples of present investigation, due to the substitution of Cr^{3+} and Cu^{2+} for Sn^{4+}, a large number of free charge carriers and oxygen vacancies might have been introduced to maintain the charge neutrality leading to the formation of BMPs. Particularly in $Sn_{0.99-x}Cu_xCr_{0.01}O_2$ (x=0.01) doped system enhanced ferromagnetism was observed, on the other hand for x≥0.01 the magnetization parameters were decreases with increasing Cu concentration, it may be due to interactions among these Cr^{3+}- Cu^{2+} and Cu^{2+}-Cu^{2+} ions becomes anti-ferromagnetic (AFM) in nature. The enhanced anti-ferromagnetic (AFM) interaction arising from the increased volume fraction of Cu ions, suppresses the ferromagnetic ordering at higher doping concentration. The values of the saturation magnetization (M_S), residual magnetization (M_R) and coercive field (H_C) of the present samples were obtained from the hysteresis loops and are given in Table 1. The table 1. indicates that the magnetization increases with the doping concentration of 1 at% of Cu and the values of saturation magnetization (M_S), residual magnetization (M_R) and coercive field (H_C) are continuously decrease with increasing doping concentration.

Table. 1 Magnetic parameters of $Sn_{0.99-x}Cu_xCr_{0.01}O_2$ (x= 0.00, 0.01, 0.03, 0.05 and 0.07) nanoparticles.

	Sample				
Parameter	x=0.00	x=0.01	x=0.03	x=0.05	x=0.07
Ms (emu/g)	23.13×10^{-3}	30.75×10^{-3}	21.31×10^{-3}	15.61×10^{-3}	10.78×10^{-3}
M_R (emu/g)	5.03×10^{-3}	29.03×10^{-4}	20.51×10^{-4}	18.66×10^{-4}	15.37×10^{-4}
Hc (Gauss)	910	640	589	540	520

IV. CONCLUSIONS

In summary, we have investigated structural, optical and magnetic properties of the chemically synthesized Cr and Cu co-doped SnO_2 DMS nanoparticles. EDAX spectra confirmed the presence of Cr and Cu in the SnO_2 host matrix. The XRD studies revealed that particles are crystallized in single phase rutile type tetragonal crystal structure ($P4_2/mnm$) of SnO_2. TEM analysis suggested the formation of nanometric particles with average particle sizes are in the range of 8-10 nm. Optical absorption spectra and corresponding Tauc's plots showed that a blueshift in optical absorption band edge and related bandgap widening with increasing Cu concentration in $Sn_{0.99-x}Cu_xCr_{0.01}O_2$ nanoparticles can be well explained in terms Burstein–Moss effect. FTIR studies recognized that strong oxide bridge functional group in all present samples. All the Cu co-doped $Sn_{0.99-x}Cu_xCr_{0.01}O_2$ nanoparticles exhibited strong room temperature ferromagnetism with nominal doping concentrations, further magnetization parameters were decreased with increasing the doping concentration. The BMP model is a reasonable explanation for observed RTFM. Hence the present synthesized material has good potential to be used in new generation spintronic devices.

V. ACKNOWLEDGMENTS

The authors are grateful to the University Grants Commission, New Delhi, Government of India, for financial support. The authors are thankful to Mr. N. Sivarama krishnan and Mr. Muttu kumar, SAIF, IIT Madras, Chennai for extending the VSM facility.

REFERENCES

1. S.A. Wolf, D.D. Awschalom, R.A. Buhrman, J.M. Daughton, S. Von Molnar, M.L. Roukes, A.Y. Chtchelkanova, D.M. Treger, "Spintronics: A Spin-Based Electronics vision for the Future", Science, vol.294, 2001, pp.1488-1495.
2. G.A. Prinz, "Magnetoelectronics", Science, vol.282 (1998) 1660-1663.
3. J. K. Furdyna, "Diluted magnetic semiconductors", J. Appl. Phys. vol.64, 1988, pp.29-64.
4. S. Datta, B. Das, "Electronic analog of the electro-optic modulator", Appl. Phys. Lett. vol.56, 1990, pp.665–667.
5. C.B. Fitzgerald, M. Venkatesan, A.P. Douvalis, S Huber, J.M.D. Coey, T. Bakas, "SnO_2 doped with Mn, Fe or Co: Room temperature dilute magnetic semiconductors", J. Appl. Phys vol.95, 2004, 7390–7392.
6. T. Dietl, H. Ohno, F. Matsukura, J. Cibert, D. Ferrand, "Zener model description of ferromagnetism in zinc-blende magnetic semiconductors", Science vol.287, 2000, pp.1019- 1022.
7. Y. Matsumoto, R. Takahashi, M. Murakami, T. Koida, X. J. Fan, T. Hasegawa, T. Fukumura, M. Kawasaki, S. Y. Koshihara, H. Koinuma, "Ferromagnetism in Co-doped TiO_2 rutile thin films grown by laser molecular beam epitaxy", Jpn. J. Appl. Phys. vol.40, 2001, pp.L1204..
8. S. N. Kale, S. B. Ogale, and S. R. Shinde, M. Sahasrabuddhe, V. N. Kulkarni, R. L. Greene T. Venkatesan, "Magnetism in cobalt-doped Cu_2O thin films without and with Al, V, or Zn codopants", Appl. Phys. Lett. vol.82, 2003, pp.2100-2102.
9. T. Fukumura, H. Toyosaki, Y. Yamada, "Magnetic oxide semiconductors", Semicond. Sci. Technol. vol.20 (2005) S103–S111.
10. W. Zeng, T. Liu, D. Liu, E. Han, "Hydrogen sensing and mechanism of M-doped SnO_2 (M=Cr^{3+}, Cu^{2+} and Pd^{2+}) nanocomposite", Sens. Actuators. B, vol.160 , 2011, pp.455–462.
11. D.S. Kumar, P.R. Carbarrocas, J.M. Siefert, "In situ invistigations of the optoelectronic properties of transparent conducting oxide/ amorphous silicon interfaces", Appl. Phys. Lett. vol.54, 1989, pp.2088–2090.
12. S. Ferrere, A. Zaban, B.A. Gregg, "Dye sensitization of nanocrystalline tin oxide by perylene derivative", J. Phys. Chem. B, vol.101, 1997, 4490–4493.
13. Y. Tachibana, K. Hara, S. Takano, K. Sayama, H. Arkawa, "Investigations on anodic photocurrent loss processes in dye sensitized solar cells: comparison between nanocrystalline SnO_2 and TiO_2 films", Chem. Phys. Lett. vol.364, 2002, pp.297–302.
14. D. Wang, S. Wen, J. Chen, S. Zhang, F. Li, Microstructure of SnO_2, Phys. Rev. B, vol.49, 1994, 14282–14285.
15. A.S.Yu, R. Frech, "Coating of multi-wall carbon nanotube with SnO2 films of controlled thickness and its applications for Li-ion battery", J. Power Sources. vol.104, 2002, pp.97-102.
16. N. Lavanya, S. Radhakrishnan, C. Sekar, M. Navaneethan, Y. Hayakawa, "Fabrication of Cr doped SnO_2 nanoparticles based biosensor for the selective determination of riboflavin in pharmaceuticals", Analyst vol.138, 2013, pp.2061–2067.
17. A.M. Abdel Hakeem, "Structure and magnetic properties of $Sn_{1-x}Mn_xO_2$", J. Magn. Magn. Mater. vol.324, 2012, pp.95–99.
18. T.R. Cunha, I.M. Costa, R.J.S. Lima, J.G.S. Duque, C.T. Meneses, "Synthesis and Magnetic Properties of Mn-Doped and SnO_2 Nanoparticles", J. Supercond. Nov. Magn.vol.26,2013, pp.2299–2302.
19. A. Punnoose, J. Hays, A. Thurber, M. H. Engelhard, R. K. Kukkadapu, C. Wang, V. Shutthanandan, S. Thevuthasan, "Development of high temperature ferromagnetism in SnO_2 and paramagnetism in SnO by Fe doping", Phys. Rev. B vol.72,2005, pp.054402-14.
20. Shendong Zhuang, XiaoyongXu, YaruPang, HeLi, BinYu, Jingguo Hu, "Variation of structural, optical and magnetic properties with Co-doping in $Sn_{1-x}Co_xO_2$ nanoparticles", J. Magn. Magn. Mater. vol.327, 2013, 24–27.
21. F.H. Aragon, J.A. H. Coaquira, P. Hidalgo, S.L.M. Brito, D. Gouvea, R.H.R. Castro, "Structural and magnetic properties of pure and Ni doped SnO_2 nanopaerticles", J. Phy. Condens. Matter. vol.22, 2010, 496003 (9pp) pp.1-9.

Published By:
Blue Eyes Intelligence Engineering
and Sciences Publication (BEIESP)

22. K. Nomura, J. Okabayashi, K. Okamura, Y. Yamada, "Magnetic properties of Fe and Co codoped SnO_2 prepared by sol-gel method", J. Appl. Phys. vol.110, 2011, 083901-4
23. Jun Okabayashi, Kiyoshi Nomura, Shin Kono, and Yasuhiro Yamada, "Magnetization Enhancement in Room-Temperature Ferromagnetic Fe–Mn Co-Doped SnO_2", Jpn. J. Appl. Phys. vol.51, 2012, pp.023003-4.
24. Jasneet kaur, Jaspreet kaur, R.K. Kotnala, Vinay gupta, Kuladeep chand varma, "Co and Fe doped SnO_2 nanorods by Ce co-doping and their electrical and magnetic properties", Adv. Mat. Lett. vol.3, 2012, pp.511-514.
25. S. Dalui, S. Rout, A.J. Silvestre, G. Lavareda, L.C.J. Pereira, P. Brogueira, O. Conde, "Structural, electrical and magnetic studies of Co: SnO_2 and (Co, Mo): SnO_2 films prepared by pulsed laser deposition", Appl. Surf. Sci. vol.278, 2013, pp.127–131.
26. K. Subramanyam, N. Sreelekha, G. Murali, D. Amaranatha Reddy, R.P. Vijayalakshmi, "Structural, optical and magnetic properties of Cr doped SnO_2 nanoparticles stabilized with polyethylene glycol",Physica B, vol.454,2014, pp.86–92.
27. L.B. Duan, X.R. Zhao, J.M. Liu, G.H. Rao, "Room temperature ferromagnetism in Cr doped ZnO nanoparticles", Appl. Phys. A, vol.99, 2010, pp.679-683.
28. Huilian Liu, Xin Cheng, Hongbo Liu, Jinghai Yang, Yang Liu, Xiaoyan Liu, Ming Gao, Maobin Wei, Xu Zhang, Yuhong Jiang, "Structural, optical and magnetic properties of Cu and V co-doped ZnO nanoparticles", Physica E vol.47,2013, pp.1–5.
29. C. Fernandez-Lopez, C. Mateo-Mateo, R.A. Alvarez-Puebla, J.P. Juste, I. P-Santos, L.M. Liz-Marzan, "Highly controlled Silica coating of PEG-capped metal nanoparticles and preparation of SERS-encoded particles", Langmuir vol.25 (24) ,2009, pp.13894–13899.
30. B.D. Cullity, "Elements of X-Ray Diffraction", Wesley, London, 1978.
31. A. Bouaine, N. Brihi, G. Schmerber, C. Ulhaq-Bouillet, S. Colis, A. Dinia, "Structural, Optical, and Magnetic Properties of Co-doped SnO_2 Powders Synthesized by the co-precipitation technique", J. Phys. Chem. C vol.111, 2007, pp.2924-2928.
32. E. Burstein, "Anomalous Optical Absorption Limit in InSb", Phys. Rev. Lett. vol.93, 1953, pp.632.
33. C. Yue-Jian, T. juan, X. Fei, Z. Jia-Bi, G. Ning, Z. Yi-Hua, D. Ye, Ge Liang, Synthesis, self-assemblyand characterization of PEG-coated iron oxide nanoparticles as potential MRI contrast agent, Drug Dev. Ind. Pharm. vol.36,2010, pp.1235–1244.
34. M. Sudha, S. Senthilkumar, R. Hariharan, A. Suganthi, M. Rajarajan, "Synthesis, characterization and study of photocatalytic activity of surface modified ZnO nanoparticles by PEG capping", J. Sol-Gel Sci. Technol. vol.65,2013, pp.301–310.
35. R. Hariharan, S. Senthil kumar, A. Suganthi, M. Rajarajan, "Synthesis and characterization of doxorubicin modified ZnO/PEG nanomaterials and its photodynamic action", J. Photochem. Photobiol. B vol.116, 2012, pp.56-65.
36. S. Gnanam, V. Rajendran, "Preparation of Cd-doped SnO_2 nanoparticles by sol–gel route and their optical properties", J Sol-Gel Sci Technol. vol.56, 2010, 128–133.
37. A. Kaminski and S. Das Sarma, "Polaron percolation in diluted magnetic semiconductors", Phys. Rev. Lett. vol.88, 2002, pp.247202-4.
38. J. M. D. Coey, M. Venkatesan and C. B. Fitzgerald, "Donor impurity band exchange in dilute ferromagnetic oxides", Nat. Mater. vol.4, 2005, pp.173-179.

Dr. R.P. Vijayalakshmi, is currently working as Associate professor at the physics department, Sri Venkateswara University, Tirupati. She received Ph.D from the same University in 1995. Her research interests are mainly: sensing applications of nanostructured devices, functional materials, nanocomposites, magnetism, multiferroics and thin Films. She published more than 50 publications in international journals.

K. Subramanyam, is a Ph.D. research scholar in the Department of physics, Sri Venkateswara University, Tirupati. He received M.Sc, from the same University. His active areas of research interest include nanostructured devices, functional materials, nanocomposites, magnetism, and thin Films.

N. Sreelekha, is a Ph.D. research scholar in the Department of physics, Sri Venkateswara University, Tirupati. She received M.Sc, from the same University. Her active areas of research interest include nanostructured devices, functional materials, nanocomposites and magnetism.

D. Amaranatha Reddy, received his Ph.D. degree in 2013 from the Department of Physics, Sri Venkateswara University in India. He is currently a Postdoctoral Fellow in the Department of chemistry at Pusan National University in South Korea. Currently he is working on the field of photochemistry especially in water treatment applications using nanostructured materials.

G.Murali, received his Ph.D. degree in 2014 from the Department of Physics, Sri Venkateswara University in India. He is currently a Postdoctoral Fellow in the Department of BIN Fusion Technology & Department of Polymer-Nano Science and Technology, Chonbuk National University, South Korea. Currently he is working on the field of Up Conversion Nanoparticles for display applications.

Published By:
Blue Eyes Intelligence Engineering and Sciences Publication (BEIESP)